International Journal of Engineering and Information Systems (IJEAIS)
ISSN: 2643-640X
Vol. 6 Issue 12, December - 2022, Pages: 57-65

Bandwidth Enhancement of a Hexagonal Microstrip Antenna using two Golf-Putter Shaped Slits in the Antenna Patch

Ali A. Rasheed, Mahmoud M. Aubais

Department of Physics, Faculty of Science, University of Kufa, Najaf, Iraq

Abstract: A hexagonal microstrip antenna that operating at a frequency of (2400MHz) was designed using (CST Studio suite 2021) program for the purpose of studying its properties (i.e. radiation pattern, bandwidth, directivity and return losses). Two slits in the patch of the shape of a golf-putter were drilled. An increase in bandwidth (1.6%-5.35%) was obtained with almost keeping the radiation pattern and directivity. Different insulating materials were used which all led to an increase in the bandwidth. In addition, the insulating material with the presence of the two slits were increased, which resulted in a slight additional improvement in the bandwidth.

Keywords: bandwidth, hexagonal microstrip antenna, finite difference in time domain method, patch drill.

Introduction

The rapid developments in the field of communications and electronics have led to the urgent need to pay special attention to microstrip antennas. It is of great importance in the communication processes, because it is the main link between outer space and the transmission line of communication devices. Its principal work lies in converting electrical signals in the transmission line into electromagnetic waves and radiating them in outer space in the case of transmission, or working to convert electromagnetic waves from outer space into electrical signals in the transmission line in the event of reception [1]. Microstrip antennas have recently become very popular because they have many advantages. This includes cheap price, ease of manufacture, lightweight, ease of installation on devices, as well as their flat appearance that microstrip arrays can be easily made [2]. Microstrip antennas operate at microwave frequencies. Therefore, it has become of great importance to researchers and workers in the field of communications and electronics. However, some disadvantages have been associated with them. For example, they include narrow bandwidth[3], which ranges between (1-2)% [4]. Efforts by telecommunications workers have been continued to increase the bandwidth of many shapes and designs of microstrip antennas [5]. One of these methods is to use dielectric materials with a low dielectric constant, but the need is to increase the dimensions of the microstrip antenna to achieve the resonant state of the same frequency [6]. The value of the dielectric constant used in most practical applications does not exceed $\varepsilon_r < 12$ [6,8,9] but, with an increase in the dielectric constant, the amount of losses increases [7,9]. Another way to increase the bandwidth is by increasing the thickness of the dielectric material, and this leads to the increase the size of the microstrip antenna, which is not desirable [8,9]. In addition, one of the methods used to increase the bandwidth is to add further patches to the main patch or to create slits in the patch or the base [10].

In this paper, we used the method of drilling the patch, where we designed a hexagonal microstrip antenna to obtain an increase in the bandwidth.

FDTD Method

A numerical method which was introduced by Kane Yee In 1966 to solve electromagnetic problems [11]. This method depends on Maxwell's curl equations, and was called finite difference time domain (FDTD) method. In this method, Yee assumed that every point in space is a cell with $\Delta x \Delta y \Delta z$ volume, and the components of $\boldsymbol{E}$ and $\boldsymbol{H}$ are distributed as shown in figure (1) [12]. Therefore, the space will become a grid of these cells. Since the electric and magnetic fields depend on the space and time, so Δt can be calculated by Courant factor as $\Delta t \leq \left(c \sqrt{\frac{1}{(\Delta x)^2} + \frac{1}{(\Delta y)^2} + \frac{1}{(\Delta z)^2}} \right)^{-1}$ where c is the light velocity.

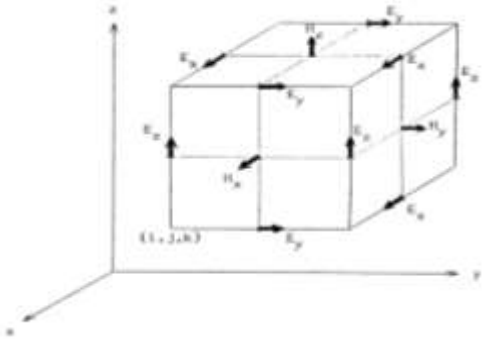

Figure 1: Yee cell in three dimensions, the dimensions of cell are Δx, Δy and Δz in x, y and z direction respectively.

The numerical updating for electric and magnetic components given as

$$H_z^{m+\frac{1}{2}}\left(i,j+\frac{1}{2},k+\frac{1}{2}\right) = \left(\frac{\mu(i,j,k)-\frac{\rho'(i,j,k)\Delta t}{2}}{\mu(i,j,k)+\frac{\rho'(i,j,k)\Delta t}{2}}\right) H_x^{m-\frac{1}{2}}\left(i,j+\frac{1}{2},k+\frac{1}{2}\right) - \frac{\frac{\Delta t}{\Delta y}}{\mu(i,j,k)+\frac{\rho'(i,j,k)\Delta t}{2}}\left(E_z^m\left(i,j,k+\frac{1}{2}\right)-E_z^m\left(i,j-1,k+\frac{1}{2}\right)\right) + \frac{\frac{\Delta t}{\Delta z}}{\mu(i,j,k)+\frac{\rho'(i,j,k)\Delta t}{2}}\left(E_y^m\left(i,j+\frac{1}{2},k\right)-E_y^m\left(i,j+\frac{1}{2},k-1\right)\right) \quad (4)$$

$$H_y^{m+\frac{1}{2}}\left(i+\frac{1}{2},j,k+\frac{1}{2}\right) = \left(\frac{\mu(i,j,k)-\frac{\rho'(i,j,k)\Delta t}{2}}{\mu(i,j,k)+\frac{\rho'(i,j,k)\Delta t}{2}}\right) H_y^{m-\frac{1}{2}}\left(i+\frac{1}{2},j,k+\frac{1}{2}\right) - \frac{\frac{\Delta t}{\Delta z}}{\mu(i,j,k)+\frac{\rho'(i,j,k)\Delta t}{2}}\left(E_x^m\left(i+\frac{1}{2},j,k\right)-E_x^m\left(i+\frac{1}{2},j,k-1\right)\right) + \frac{\frac{\Delta t}{\Delta x}}{\mu(i,j,k)+\frac{\rho'(i,j,k)\Delta t}{2}}\left(E_z^m\left(i,j,k+\frac{1}{2}\right)-E_z^m\left(i-1,j,k+\frac{1}{2}\right)\right) \quad (5)$$

$$H_z^{m+\frac{1}{2}}\left(i+\frac{1}{2},j+\frac{1}{2},k\right) = \left(\frac{\mu(i,j,k)-\frac{\rho'(i,j,k)\Delta t}{2}}{\mu(i,j,k)+\frac{\rho'(i,j,k)\Delta t}{2}}\right) H_z^{m-\frac{1}{2}}\left(i+\frac{1}{2},j+\frac{1}{2},k\right) - \frac{\frac{\Delta t}{\Delta x}}{\mu(i,j,k)+\frac{\rho'(i,j,k)\Delta t}{2}}\left(E_y^m\left(i,j+\frac{1}{2},k\right)-E_x^m\left(i-1,j+\frac{1}{2},k\right)\right) + \frac{\frac{\Delta t}{\Delta y}}{\mu(i,j,k)+\frac{\rho'(i,j,k)\Delta t}{2}}\left(E_x^m\left(i+\frac{1}{2},j,k\right)-E_z^m\left(i+\frac{1}{2},j-1,k\right)\right) \quad 6$$

$$E_x^{m+1}\left(i+\frac{1}{2},j,k\right) = \left(\frac{\varepsilon(i,j,k)-\frac{\sigma(i,j,k)\Delta t}{2}}{\varepsilon(i,j,k)+\frac{\sigma(i,j,k)\Delta t}{2}}\right) E_x^m\left(i+\frac{1}{2},j,k\right) + \frac{\frac{\Delta t}{\Delta y}}{\varepsilon(i,j,k)+\frac{\sigma(i,j,k)\Delta t}{2}}\left(H_z^{m+\frac{1}{2}}\left(i+\frac{1}{2},j+\frac{1}{2},k\right)-H_z^{m+\frac{1}{2}}\left(i+\frac{1}{2},j-\frac{1}{2},k\right)\right) - \frac{\frac{\Delta t}{\Delta z}}{\varepsilon(i,j,k)+\frac{\sigma(i,j,k)\Delta t}{2}}\left(H_y^{m+\frac{1}{2}}\left(i+\frac{1}{2},j,k+\frac{1}{2}\right)-H_y^{m+\frac{1}{2}}\left(i+\frac{1}{2},j,k-\frac{1}{2}\right)\right) \quad 7$$

$$E_y^{m+1}\left(i,j+\frac{1}{2},k\right) = \left(\frac{\varepsilon(i,j,k)-\frac{\sigma(i,j,k)\Delta t}{2}}{\varepsilon(i,j,k)+\frac{\sigma(i,j,k)\Delta t}{2}}\right) E_y^m\left(i,j+\frac{1}{2},k\right) + \frac{\frac{\Delta t}{\Delta z}}{\varepsilon(i,j,k)+\frac{\sigma(i,j,k)\Delta t}{2}}\left(H_x^{m+\frac{1}{2}}\left(i,j+\frac{1}{2},k+\frac{1}{2}\right)-H_x^{m+\frac{1}{2}}\left(i,j+\frac{1}{2},k-\frac{1}{2}\right)\right) - \frac{\frac{\Delta t}{\Delta x}}{\varepsilon(i,j,k)+\frac{\sigma(i,j,k)\Delta t}{2}}\left(H_z^{m+\frac{1}{2}}\left(i+\frac{1}{2},j+\frac{1}{2},k\right)-H_z^{m+\frac{1}{2}}\left(i-\frac{1}{2},j+\frac{1}{2},k\right)\right) \quad 9$$

$$E_z^{m+1}\left(i,j,k+\frac{1}{2}\right) = \left(\frac{\varepsilon(i,j,k)-\frac{\sigma(i,j,k)\Delta t}{2}}{\varepsilon(i,j,k)+\frac{\sigma(i,j,k)\Delta t}{2}}\right) E_z^m\left(i,j,k+\frac{1}{2}\right) + \frac{\frac{\Delta t}{\Delta x}}{\varepsilon(i,j,k)+\frac{\sigma(i,j,k)\Delta t}{2}}\left(H_y^{m+\frac{1}{2}}\left(i+\frac{1}{2},j,k+\frac{1}{2}\right)-H_x^{m+\frac{1}{2}}\left(i-\frac{1}{2},j,k+\frac{1}{2}\right)\right) - \frac{\frac{\Delta t}{\Delta y}}{\varepsilon(i,j,k)+\frac{\sigma(i,j,k)\Delta t}{2}}\left(H_x^{m+\frac{1}{2}}\left(i,j+\frac{1}{2},k+\frac{1}{2}\right)-H_x^{m+\frac{1}{2}}\left(i,j-\frac{1}{2},k-\frac{1}{2}\right)\right) \quad 10$$

Where $\varepsilon(i,j,k)$,$\mu(i,j,k)$,$\sigma(i,j,k)$, and $\rho'(i,j,k)$ are the permittivity, permeability, electric conductivity, and magnetic conductivity at point (i,j,k)

The excitation of the system can be done by Gausses pulse[11] .

$$p(t) = e^{-\left(\frac{t-t_0}{\tau}\right)^2}$$

where τ is the damping factor and its value depends on the frequency range of problem, and t_0 is the time delay.

The pulse must propagated as described in the equation above. Since the memory of the computer cannot programing infinity space, a model to simulate the infinite space was used. This model is complex frequency-shifted Perfectly Matched Layer (CFS-PML) [11].

When the electric and magnetic fields updating approach to zero at feed point, one can calculate the input impedance Zin and $S11$ as follows:

$$Z_{in}(\omega) = \left(\frac{\int_{-\infty}^{\infty} V(t)e^{-j\omega t}dt}{\int_{-\infty}^{\infty} I(t)e^{-j\omega t}dt}\right) = \frac{\sum_{m=0}^{M} V(m\Delta t)e^{-j\omega m\Delta t}\Delta t}{\sum_{m=0}^{M-1} I\left(\left(m+\frac{1}{2}\right)\Delta t\right)e^{-j\omega\left(m+\frac{1}{2}\right)\Delta t}\Delta t}$$

$$S_{11} = \left(\frac{\int_{-\infty}^{\infty} V(t)e^{-j\omega t}dt}{\int_{-\infty}^{\infty} p(t)e^{-j\omega t}dt}\right)$$

Where $V(t)$ is the voltage in the time domain at the feed point. calculated by Faraday's law given as

$$V_{feed}^{M} = -\frac{1}{u-b}\left(\sum_{i=i_{feed}-1}^{i=i_{feed}+1}\sum_{j=j_{feed}-1}^{j=j_{feed}+1}\sum_{k=b}^{k=u} E_z^m\left(i_{feed}, j_{feed}, k\right)\Delta z\right)$$

and $I(t)$ is the current in the time domain at feed point. calculated by Ampere's law that given as

$$I(t) = \frac{1}{u-b}\left(\sum_{k=b}^{k=u}\left(\sum_{i=i_{feed}-1}^{i=i_{feed}+1} H_x^{m+\frac{1}{2}}(i,j-1,k)\Delta x + \sum_{j=j_{feed}-1}^{j=j_{feed}+1} H_y^{m+\frac{1}{2}}(i-1,j,k)\,\Delta y - \sum_{i=i_{feed}-1}^{i=i_{feed}+1} H_x^{m+\frac{1}{2}}(i,j+1,k)\Delta x - \sum_{j=j_{feed}-1}^{j=j_{feed}+1} H_y^{m+\frac{1}{2}}(i+1,)\,\Delta y\right)\right)$$

and $p(t)$ is the Gaussian pulse at feed point. Then, we were calculated the other properties of system.

Calculations and results:

A hexagonal microstrip antenna was designed, in which the base and patch were made of copper and the insulating material (Rogers Diclod87) with a dielectric constant of ($\varepsilon_r = 2.33$) to operate at a resonant frequency (2400MHz), it was fed by a coaxial feed at the point ($R_f = (7,0)$ mm) from the center of the patch as shown in Figure (2). The dimensions of the microstrip antenna can be seen in Table (1).

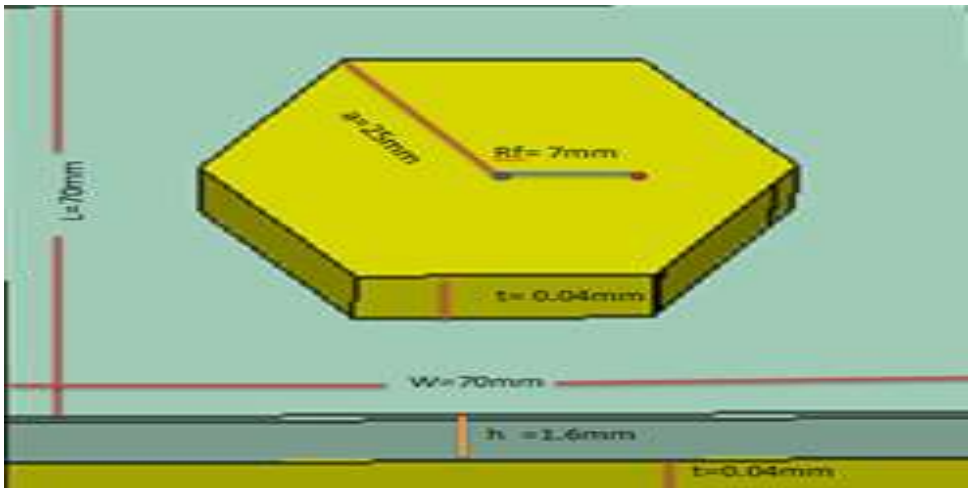

Figure (2) Hexagonal microstrip antenna with its dimensions.

Table (1) Dimensions of the hexagonal microstrip antenna

A	25 mm

W	70 mm
L	70 mm
T	0.04 mm
H	1.6 mm

For the antenna to work efficiently, the input impedance must be matched to be 50Ω at the resonant frequency. Figure (3) demonstrates the resistance and reactance against the frequency.

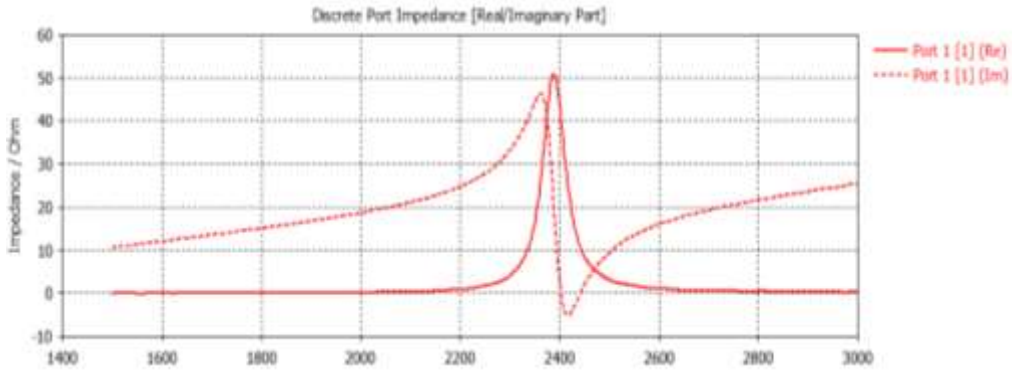

Figure (3): The input impedance against frequency calculated by FDTD method

$$"a = 25\ mm,, h = 1.6\ mm\ , \varepsilon_r = 2.33, \qquad R_f = (7\ , 0)mm$$

Figure (4) shows the change of return losses S_{11} against frequency, and the bandwidth was calculated according to the equation below [7].

$$BW = \frac{2(f_{max} - f_{min})}{f_{max} + f_{min}}\ 100\%$$

where f_{min} and f_{max} are the frequencies values at which $S_{11} = -10$ dB. The bandwidth was found to be approximately 1.6%.

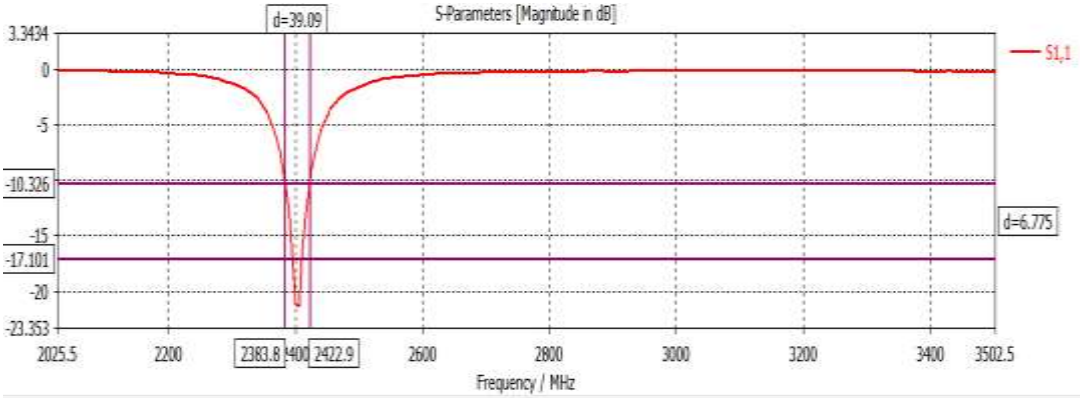

Figure (4): The return loss S_{11} of the hexagonal microstrip antenna that calculated by the FDTD method.

$$"a = 25\ mm\ , h = 1.6\ mm\ , \varepsilon_r = 2.33,\ ,\ R_f = (7\ , 0)mm".$$

Two slits were drilled in the patch of the microstrip antenna as shown in Figure (5), and Table (2) demonstartes the dimensions of the slits.

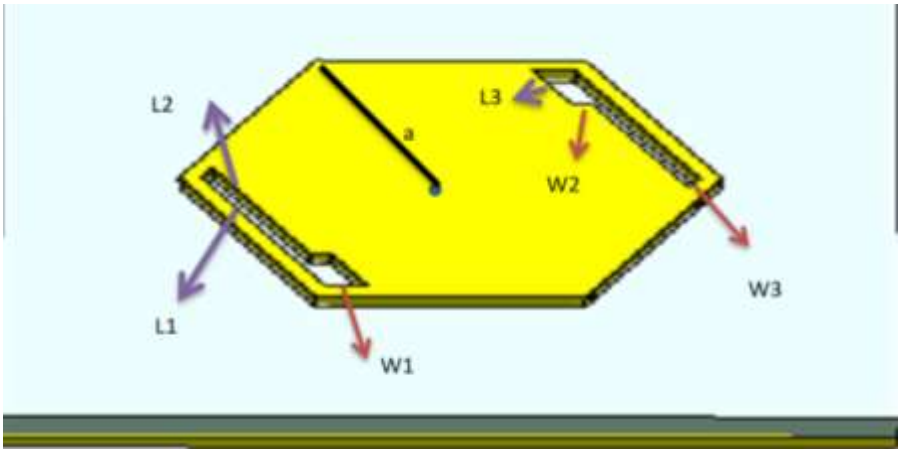

Figure (5): shows the shape of the cracks in the patch of the microstrip antenna.

Table (2): represents the dimensions of the slits in the patch of the hexagonal microstrip antenna (SHMSA).

L1	21mm	W1	5 mm
L2	13mm	W3	3.5mm
L3	9mm	W3	1.5mm

Figure (6) shows the return losses (S_{11}) compared to the frequency of the two-slit microstrip antenna, from which the bandwidth was calculated, where its value became (4.61dB).

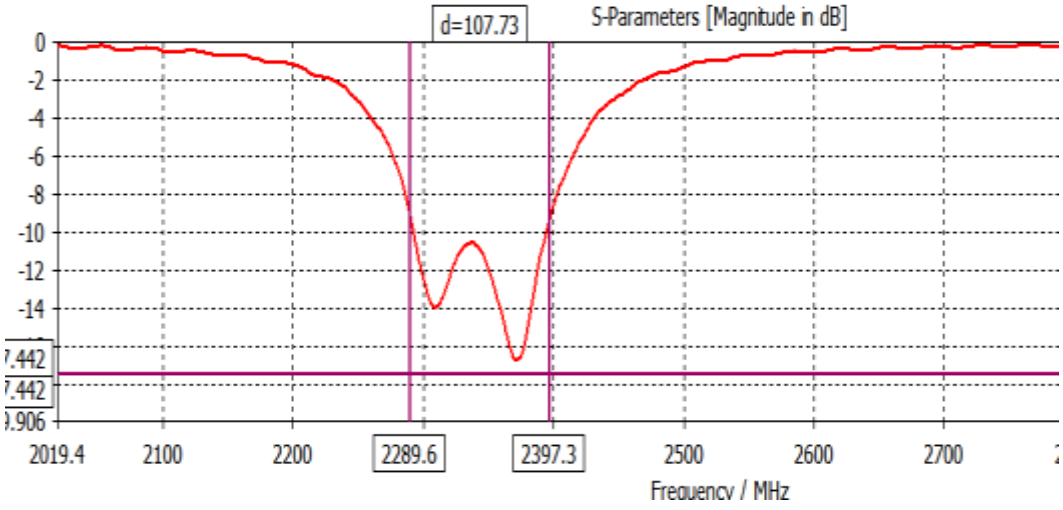

Figure (6): return loss S_{11} of a two-slit hexagonal microstrip antenna calculated by FDTD method.

$$a = 25\ mm, \varepsilon_r = 2.33,\ R_f = (12\ , -1)mm$$

The radiation pattern was found, and it was preserved without any change. As for the directivity, a slight change in the directivity occurred when cracks occurred in the patch. Figure (7) shows the radiation pattern after drilling the two slits in the patch.

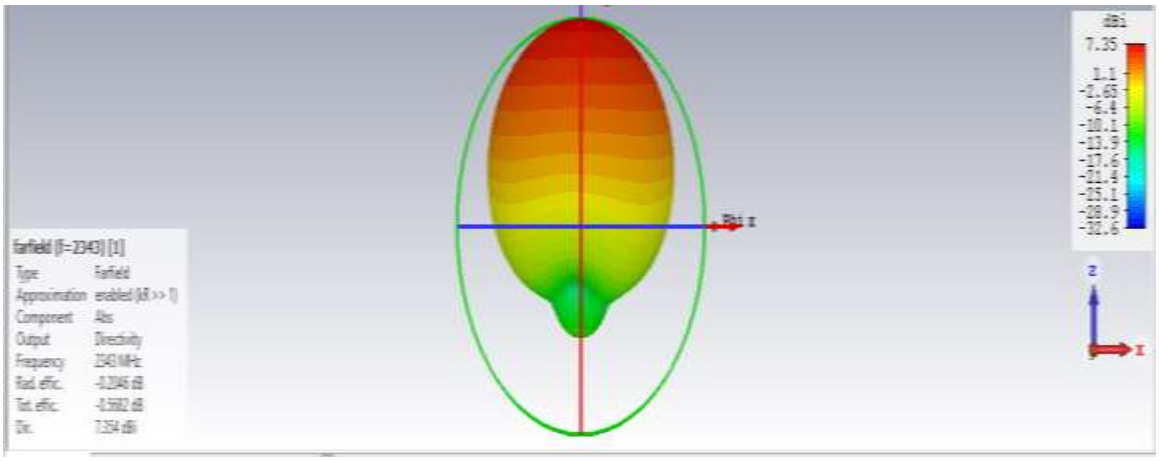

Figure (7): The radiation pattern of the hexagonal microstrip antenna engraved with two slits on the patch. The results were obtained using the method (FDTD)

The same procedures were applied to the same dielectric substance material with different heights, and the results are shown in the table below (3)

Table (3) shows the results we obtained by drilling the patch and increasing the height of the dielectric substance material

	h mm	F2-f1 MHz	fo MHz	BW%	Dir dB
HMSA	1.6	39	2400	1.6	**7.4**
	2	48	2396	2	**7.387**
	3	61.5	2388	2.58	**7.38**
SHMSA	1.6	108	2393	4.61	**7.33**
	2	118	2366	5	**7.31**
	3.2	124	2306	5.38	**7.29**

The other dielectric materials were used with different dielectric constants to design hexagonal microstrip antennas. It also operates at a resonant frequency (2400MHz). slits were drilled in the patch with the same slits shapes as shown in Figure (5), but with different dimensions. The same calculations were performed, where Table (4) presents the results which were obtained using the FDTD method.

Table (4): The results we obtained by drilling cracks in the patch with the change in height and type of insulating material.

		A mm	h mm	Δf *MHZ*	f_0 MHZ	BW%	DIR dB
RT5880LZ Rogers ε_r=2	HMSA	27	1.6	42	2400	1.75	7.61
			3.2	64	2330	2.75	7.54
	SHMSA		1.6	108	2333	4.7	7.6
			3.2	127	2298	5.53	7.54
Rogers Diclod87 ε_r =2.33	HMSA	25	1.6	39	2400	1.6	7.4
			3.2	61.5	2388	2.58	7.38
	SHMSA		1.6	108	2393	4.61	7.33
			3.2	124	2306	5.38	7.29
Rogers xt8000 ε_r=3.3	HMSA	21	1.6	36	2400	1.5	7.03
			3.2	59	2345	2.5	6.93
	SHMSA		1.6	88	2373	3.75	7.02
			3.2	97	2335	4.13	6.95
Preperml440 ε_r=4.4	HMSA	18	1.6	33	2400	1.37	6.515

			3.2	57	2374	2.4	6.45
	SHMSA		1.6	82	2403	3.41	6.804
			3.2	88	2354	3.74	6.69

Conclusions

After designing a hexagonal microstrip antenna which made of copper and the insulating material which is (Rogers Diclod87), and after digging slits in the patch, we noticed an increase in the bandwidth from 1.6% to 4.61%, with the radiation pattern remaining unchanged further to a slight change in directivity. The improvement in bandwidth occurs due to the occurrence of additional surface currents around the cracks, which increases the radiated power, and thus increases the quality factor Q, and thus increases the bandwidth. Increasing the thickness of the insulating material can also lead to an increase in the bandwidth and it reached 5.38% while keeping the same cracks dimensions. After using a dielectric material with a low dielectric constant, a further increase in bandwidth was obtained.

References

[1]RASI, M. "WIDEBAND APERTURE COUPLED MICROSTRIP PATCH ARRAY ANTENNA." (2019).
[2] D. Colles and D. Arakaki, "Multi-technique broadband microstrip patch antenna design," *2014 IEEE Antennas and Propagation Society International Symposium (APSURSI)*, 2014, pp. 1879-1880, doi: 10.1109/APS.2014
[3] Bhunia, Sunandan. (2013). Microstrip Patch Antenna's Limitations and some Remedies. IJECT
[4] Balanis, C. A. (2015). Antenna theory: analysis and design. John wiley & sons.
[5] Roy, A. A., Môm, J. M., & Kureve, D. T. (2013, November). Effect of dielectric constant on the design of rectangular microstrip antenna. In 2013 IEEE International Conference on Emerging & Sustainable Technologies for Power & ICT in a Developing Society (NIGERCON) (pp. 111-115)
[6] Aastha, A. Kaur, A. S. Dhillon and E. Sidhu, "Performance analysis of microstrip patch antenna employing Acrylic, Teflon and Polycarbonate as low dielectric constant substrate materials," 2016 International Conference on Wireless Communications, Signal Processing and Networking (WiSPNET), 2016, pp. 2090-2093, doi: 10.1109/WiSPNET.2016.7566510.
[7] Kumar, G., & Ray, K. P. (2002). Broadband microstrip antennas. Artech house.
[8] Z. A. Hassoun, M. H. Wali, H. A. Hussein, N. H. Haroon and A. Alkhayyat, "Study the Effect of Dielectric Permittivity and Changing Substrates Material on Microstrip Patch Antenna," 2022 International Congress on Human-Computer Interaction, Optimization and Robotic Applications (HORA), 2022, pp. 1-5
[9]Rop. PhD, K.V. & Konditi, Dominic. (2012). PERFORMANCE ANALYSIS OF A RECTANGULAR MICROSTRIP PATCH ANTENNA ON DIFFERENT DIELECTRIC SUBSTRATES. International Institute for Science, Technology and Education (IISTE). 3. 7-14.
[10] Usha Kiran, K., Yadahalli, R.M., Vani, R.M. and Hunagund, P.V. (2008) Compact Broadband Stacked Dual Wide Slit Loaded Rectangular Microstrip Antenna. Radio and Space Physics, 37, 366-369
[11] Elsherbeni, A. Z., & Demir,V.(2015). The finite-difference time-domain method for electromagnetics with MATLAB® simulations (Vol. 2). IET
[12] Kraeck and I. Hahn, "Finite-difference time-domain (FDTD) algorithm for multiblock grids," 2014 International Conference on Electrical Machines (ICEM), 2014, pp. 1179- 1185, doi: 10.1109/ICELMACH.2014.6960331.